

EINDHOVEN UNIVERSITY OF TECHNOLOGY

2IMV20

VISUALIZATION

Assignment 1: VolVis

Group 28:
Martin ter Haak (0846351)
Jelle van Miltenburg (1195537)

December 11, 2016



Contents

1	Introduction	3
2	Theory & Methods	4
2.1	Ray casting	4
2.1.1	Tri-linear interpolation	4
2.1.2	Slicer	4
2.1.3	MIP	5
2.1.4	Compositing	5
2.1.5	Responsiveness improvement	6
2.2	2-D transfer functions	6
2.2.1	Extension triangle widget	7
2.2.2	Phong shading	8
3	Data exploration	10
3.1	Piggy bank	10
3.1.1	Slicer	10
3.1.2	MIP	11
3.1.3	Compositing	11
3.1.4	2-D Transfer function	11
3.1.5	Main findings	12
3.2	Backpack	12
3.2.1	Slicer	12
3.2.2	MIP	12
3.2.3	Compositing	12
3.2.4	2-D transfer function	13
3.2.5	Main findings	14
3.3	Torso	14
3.3.1	Slicer	14
3.3.2	MIP	15
3.3.3	Compositing	15
3.3.4	2-D transfer function	16
3.3.5	Main finding	16
4	Results & Conclusion	17
5	Discussion	18

6 Appendix	19
6.1 Parameter settings	19

Chapter 1

Introduction

Advances in three-dimensional digital imaging techniques caused an increase in the generation of spatial volume sets [1, 5, 6] (Truernit et al., 2008; Fernandez et al., 2010; Kierzkowski et al., 2012; Roeder et al., 2012). As a response, the number of volume rendering techniques increased accordingly [2](Meißer et al, 2000). These techniques strive to valorize the spatial volume data by displaying the volumetric data in a meaningful two-dimensional image. This should make it possible to answer different questions, like ‘What does the data represent?’, ‘Are there different objects identifiable?’ and ‘Which irregularities are shown in the data?’. However, different data sets and different questions require different volume rendering techniques. The new challenge is to select the appropriate technique in different contexts. The goal of this paper is to develop and compare several volume rendering techniques and conclude advantages and disadvantages of the different technique in different contexts. Since the techniques score is based on several factors, the different techniques will be ranked on different performance indicators. It is easy to imagine that the performance is dependent on the responsiveness of the tool, as well as the ability to distinguish different items. Furthermore, it might be necessary to look at what the data represents as a whole. Also, it adds value to the performance if a user has a lot of control over what is displayed. Lastly, the visibility of the surface is sometimes important. We therefore ranked the techniques on performance indicators ”visibility of surface”, ”distinguishable items”, ”showing bigger picture”, ”responsiveness”, ”view control”.

In this paper, we extend on a number of different volume rendering techniques based on a raycasting approach. First, we briefly discuss a technique called ‘slicing’. We did not develop this technique, but we use it for data exploration and as a foundation for other techniques. Secondly, we discuss the development of ‘tri-linear interpolation’, ‘Maximum Intensity Projection (MIP)’, ‘compositing’, and finally we discuss ‘2-D transfer functions’. After the theoretical extension, we perform a data exploration on different data sets, using developed techniques. We end our paper with a conclusion of the different volume rendering techniques.

Chapter 2

Theory & Methods

2.1 Ray casting

This section will describe the different methods towards a volume rendering technique that uses ray casting. First it describes the tri-linear interpolation trick that can be used to calculate the voxel intensities more accurately. Then it explains the volume rendering techniques slicer, Maximum Intensity Projection and the compositing. Lastly, the improvement of the responsiveness is described.

2.1.1 Tri-linear interpolation

The initial implementation of the function that gets the voxel intensity value for given x , y and z , simply rounded the coordinates down and returned value for that voxel. This is, however, crude since it simply ignores the values of the other surrounding voxels when x , y or z are not natural numbers but float between multiple voxels. To also account for these values we need to use tri-linear interpolation. For this we used the following calculation:

$$\begin{aligned}x_0, y_0, z_0 &\leftarrow \lfloor x \rfloor, \lfloor y \rfloor, \lfloor z \rfloor \\x_1, y_1, z_1 &\leftarrow \lceil x \rceil, \lceil y \rceil, \lceil z \rceil \\\alpha, \beta, \gamma &\leftarrow x - x_0, y - y_0, z - z_0 \\S_{xyz} &\leftarrow (1 - \alpha)(1 - \beta)(1 - \gamma) * S_{000} + \alpha(1 - \beta)(1 - \gamma) * S_{100} + (1 - \alpha)\beta(1 - \gamma) * S_{010} + \alpha\beta(1 - \gamma) * S_{110} + (1 - \alpha)(1 - \beta)\gamma * S_{001} + \alpha(1 - \beta)\gamma * S_{101} + (1 - \alpha)\beta\gamma * S_{011} + \alpha\beta\gamma * S_{111}.\end{aligned}$$

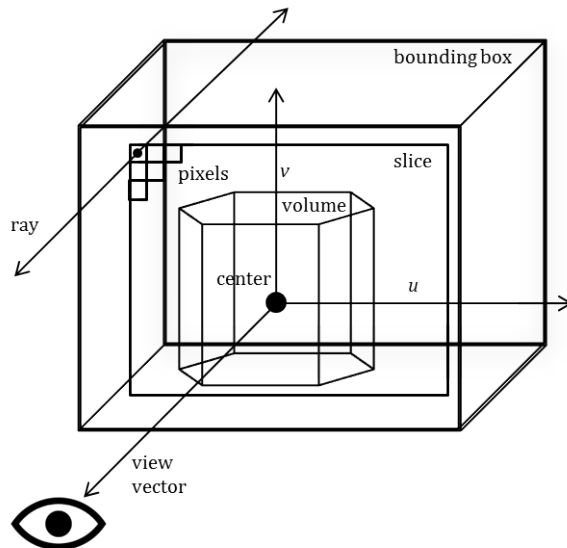
Here S_{xyz} denotes the final tri-linear interpolated value. S_{000} denotes the value at x_0, y_0, z_0 and S_{101} the value at x_1, y_0, z_1 for example.

This approach was taken from the lecture notes Spatial data I.

2.1.2 Slicer

Although the volume rendering technique slicer was already implemented in the assignment we still want to explain it. Essentially the slicer displays only a single slice through the object that cuts through the center and is perpendicular to the view vector. On this slice each voxel is displayed using a grayscale color that linearly correlates with its intensity. This

Figure 2.1: Raycasting



way of visualizing is very fast and nice to quickly get an overview of the contents of some object. However it can not be used for analyzing surfaces and it is hard to examine the other contents that are far from the center. For this reason we will be implementing more advanced techniques of volume rendering.

2.1.3 MIP

Maximum Intensity Projection (MIP) is a technique that uses raycasting to render a volume. Raycasting means shooting a ray through the volume for each pixel in the image and considering all the voxels along the ray when determining the color of the pixel.

For MIP we reused the code of the slicer. For ray casting we can shoot a ray from the plane of the slice in both directions parallel to the view vector (see Figure 2.1). The length in both directions is equal to $\frac{1}{2}\sqrt{(V_{dimX})^2 + (V_{dimY})^2 + (V_{dimZ})^2}$. V_{dimX} , V_{dimY} , V_{dimZ} are the sizes of the volume in the x , y and z dimension respectively. With this distance we can be sure that no voxels are missed because this makes the rays the same length as the diagonal of the cube. The voxels outside of the volume are not considered.

Since we are doing Maximum Intensity Projection we need to return, for each pixel, the maximum value of all voxels encountered on the ray. This value is then divided by the maximum value of all the voxels in the volume and linearly converted to a grayscale color.

2.1.4 Compositing

Compositing is also a method of volume rendering that uses raycasting. But, while MIP only shows the value with the highest intensity along a ray, this technique makes a color composite of all the values along the ray. Starting from the point on the ray that is furthest from the

Figure 2.2: Levoy's alpha calculation function

$$\alpha(\mathbf{x}_i) = \alpha_v \begin{cases} 1 & \text{if } |\nabla f(\mathbf{x}_i)| = 0 \text{ and } \\ & f(\mathbf{x}_i) = f_v \\ 1 - \frac{1}{r} \left| \frac{f_v - f(\mathbf{x}_i)}{|\nabla f(\mathbf{x}_i)|} \right| & \text{if } |\nabla f(\mathbf{x}_i)| > 0 \text{ and } \\ & f(\mathbf{x}_i) - r |\nabla f(\mathbf{x}_i)| \leq f_v \leq \\ & f(\mathbf{x}_i) + r |\nabla f(\mathbf{x}_i)| \\ 0 & \text{otherwise} \end{cases}$$

viewer, it iteratively draws the color of the next point over the point behind it. If the current point has an alpha value lower than 1 this means it will show part of the voxel(s) behind it. The formula is:

$$\text{color} = \text{alpha}_i * \text{color}_i + \text{alpha}_i * \text{color}_{i-1}$$

where i denotes the current point and $i - 1$ the previous point behind it

The *alpha* and *color* for a given voxel depend on its intensity and can be calculated using a 1D transfer function. The application already provides an interface to edit this function. It is possible to set the color and opacity for a number of different intensities. The transfer function can then determine the color and opacity for a certain intensity by applying linear interpolation.

2.1.5 Responsiveness improvement

Rendering the volume using raycasting is quite slow. In full resolution rendering can take more than 2 seconds. Therefore we have decided to render the volume in a lower resolution during interaction for MIP and compositing, in other words while moving the trackball. The lower resolution is achieved by calculating the color for only some of the pixels and then coloring a number of surrounding pixels with the same color. Since less calculations are needed to determine the colors of the pixels, rendering is faster.

During interaction a square of 3×3 pixels are colored with the same color. In particular they get the color of the center pixel. If the user does not move the trackball for 1 second, then the volume is rerendered but now on full resolution. So the color of each pixel is calculated and shown separately. This trick allows the user to first rotate the object without delay such that it provides a good view. Then after releasing the trackball the application renders the object in full resolution.

2.2 2-D transfer functions

Being able to render volumes using a 1D transfer function is nice because you can set the color and opacity for different intensities. The paper *Multi-Dimensional Transfer Functions for Interactive Volume Rendering* [4] however argues that "Often, there are features of interest in volume data that are difficult to extract and visualize with 1D transfer functions". Marc Levoy recognised the same problem and devised a method of incorporating gradient-based

opacity weighting in compositing [3]. He proposed to use the function in Figure 2.2 to calculate the opacity of each voxel.

In this function the variables are as follows:

- α_v , the desired overall opacity
- r , the desired thickness of the transition region
- f_v , the desired intensity at the center of the transition region
- $f(x_i)$, the intensity of the voxel
- $|\nabla f(x_i)|$, the gradient magnitude at the voxel

The parameters α_v , r and f_v can be set using the given triangle widget in the application. f_v is directly retrieved from the volume data representation. The gradient magnitude is calculated as follows:

For a certain voxel i with coordinates (x_i, y_i, z_i) :

$$|\nabla f(i)| = \sqrt{(0.5(f(x_{i+1}, y_i, z_i) - f(x_{i-1}, y_i, z_i)))^2 + (0.5(f(x_i, y_{i+1}, z_i) - f(x_i, y_{i-1}, z_i)))^2 + (0.5(f(x_i, y_i, z_{i+1}) - f(x_i, y_i, z_{i-1})))^2}$$

while this is not the exact gradient magnitude it is a very close estimation.

Furthermore the voxel intensities $f(x_i)$ are all tri-linearly interpolated as described in the subsection *Tri-linear interpolation*. We found this did not impair the speed of the application.

2.2.1 Extension triangle widget

Using the given triangle widget we can now set the parameters region r , opacity α_v and the base intensity f_v of Levoy's method of volume rendering. The triangle can be moved horizontally to set f_v and the width of the base can be changed to set r . By doing this different curves and therefore different surfaces can be targeted. This however does not provide enough freedom to select only certain parts of a curve. To allow more flexibility another paper suggests to add the option of shearing along the gradient magnitude axis, "so that higher values are emphasized at higher gradients, allows us to follow the center of some boundaries more accurately" [4].

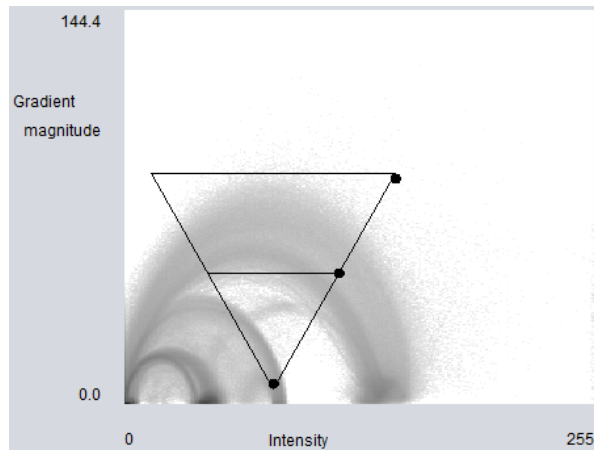
We have taken this advice and added three more parameters, namely:

- *baseGradientMagnitude*, the gradient magnitude at the lowest point of the triangle
- *minGradientMagnitude*, the gradient magnitude at the bottom of the shear
- *maxGradientMagnitude*, the gradient magnitude at the top of the triangle

These can be set using the triangle widget by dragging any of the dots in the gradient magnitude dimension. As can be seen in Figure 2.3 this allows us to focus on only a part of a curve.

The three new parameters are used as following in the Levoy's alpha function. When the gradient magnitude is smaller than the *minGradientMagnitude* or larger than *maxGradientMagnitude*,

Figure 2.3: Extended triangle widget



then $\alpha(x_i) = 0$ is returned. If not, then the *baseGradientMagnitude* is subtracted from $|\nabla f(x_i)|$ and Levoy's function is applied.

2.2.2 Phong shading

Using Levoy's 2D transfer function we can visualize surfaces quite nicely as can be seen in Figure 2.4a. Yet it is still hard to distinguish depth in the image because no shading is applied. In other words, all the faces get the same color while they may be differently orientated in respect to the viewer. This makes it difficult to see where transitions to different faces take place. Ideally you would want to place a virtual light on the object so that distinct faces light up differently.

To achieve this the Phong shading model can be used which is popular due to its simplicity and computational speed. The simplified Phong model uses the following formula:

$$I = I_a + I_d k_{diff}(L \cdot N) + k_{spec}(N \cdot H)^\alpha \text{ with } H = \frac{L+V}{|L+V|}$$

The Wikipedia article provides a nice explanation of the theory and discusses the parameters [7].

We used the following parameters: $I_a = 0.1$, $I_d = 1.0$, $k_{diff} = 0.7$, $k_{spec} = 0.2$ and $\alpha = 10$ as suggested in the assignment. Furthermore we made the assumption that the light source is exactly located at the viewpoint so $L = V$. Also $V = -viewVector$ and $N_i = -\nabla f(x_i)$. Now that we have the shading coefficient I which is a number between 0 and 1, we can simply multiply this with the color of the voxel to find its color with shading applied. Using these parameters we get the result in Figure 2.4b. As you can see with shading the flower pattern is much easier to distinguish.

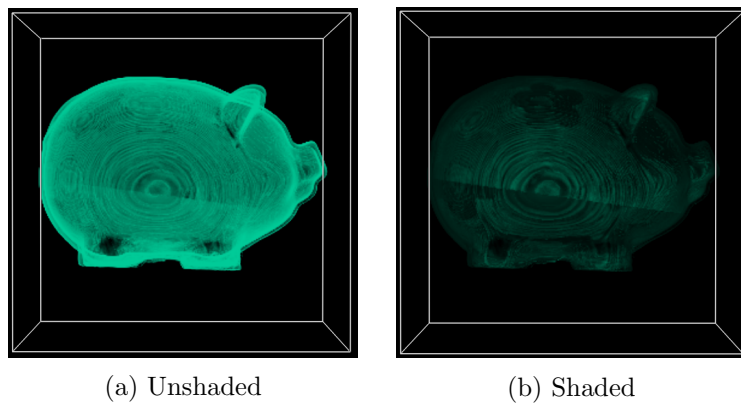


Figure 2.4: Unshaded and shaded version of the piggy bank.

Chapter 3

Data exploration

The developed application can be used to explore 3-D data sets that represent a volume. Several data sets are explored to test and compare the different rendering techniques on their performance. Three of these data sets gave some interesting insights and are discussed in this section. For every data set, we first apply the four different techniques and we conclude with the main findings. All explorations are enriched with images. The parameter settings are shown in the appendix, in case of the rendering techniques that require parameter settings.

3.1 Piggy bank

3.1.1 Slicer

A slice through the middle of this piggy bank reveals a hole in the top and one at the bottom (Figure 3.1a). The one at the bottom, however, is closed with an object, consisting of harder and softer materials. The slicer also displays a number of round objects, presumably coins.

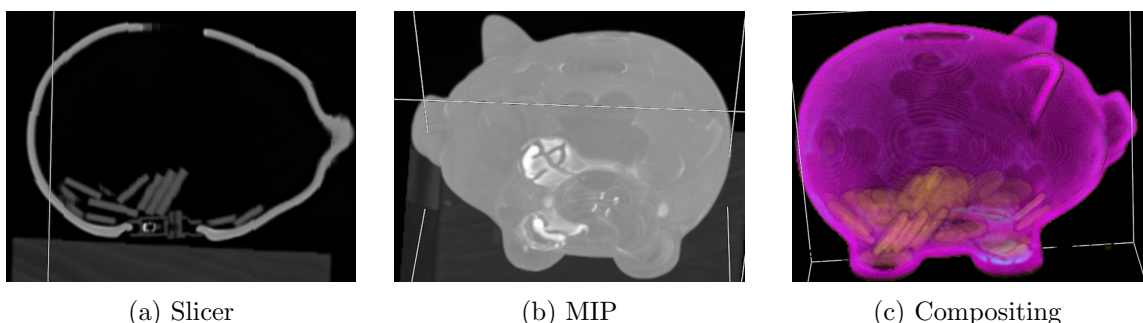


Figure 3.1: Ray casting volume rendering results of a piggy bank.

3.1.2 MIP

The MIP shows that the stopper in the belly of the piggy pig has four hard, maybe metal, rings (Figure 3.1b). Also, a hard material is spread out in the front feet of the pig. It is striking that the coins are not visible anymore. A metal coin is harder than a clay piggy bank. This indicates that the coin shapes might not be real coins.

3.1.3 Compositing

The compositing technique requires the user to set parameters. The user is guided through this process by the "opacity-scalar value" graph. Tediously, the best strategy is trial and error. After a couple of tries, we found a convincing transfer function that creates a nice view of the outside of the piggy bank. The flowers on the outside of the piggy bank are now visible. A few tries later, we found a set of parameters that showed the inside of the piggy bank. We can estimate that the animal contains around 25 coins. It is remarkable that the coins have a lower intensity than both the piggy bank and the four pins in the stopper. Presumably this means that the coins are not made out of metal and might be plastic, chocolate, or another softer material. We can only conclude this if we assume that the 'intensity' is directly linked to the density of the material, which is not completely clear. The result of compositing rendering can be seen in Figure 3.1c. The parameter settings can be found in the appendix.

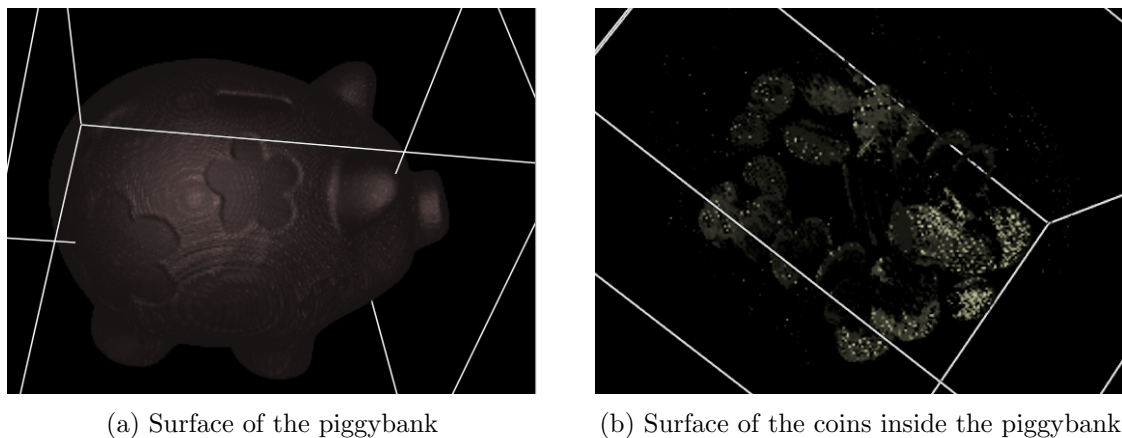


Figure 3.2: 2-D Transfer function volume rendering results of a piggy bank.

3.1.4 2-D Transfer function

The 2-D transfer function also, like compositing, requires adjustments on the parameters. This time, a "gradient magnitude - intensity" graph can be used as guide through this process. We also checked on the shading effect, to get the best results. After trial en error,

the parameters are set in a way that the surface of the piggy bank is nicely visualized. We notice that the piggy bank is indeed covered with a flower pattern (Figure 3.2a). When the parameters are set properly, it is also possible to visualize the coins inside the piggy bank, but this does not add much to the previous rendering techniques (Figure 3.2a). The parameter settings are shown in the appendix.

3.1.5 Main findings

Although a piggy bank is usually used to store money, this piggy bank is probably used to store fake money. The coins show a lower intensity than the piggy bank itself. This could mean that the coins inside are no real coins, but rather consist of a softer material like plastic or chocolate. It is not completely clear, however, if the intensity value is directly linked to the density of a material.

3.2 Backpack

3.2.1 Slicer

In this context, the slicer does not give a nice representation of the data. The data set represents a backpack with different objects inside (Figure 3.3a). A slicer is not the best way to visualize such an object. Surprisingly, it shows a lighter. This lighter was not clearly visible using MIP and compositing.

3.2.2 MIP

The MIP slightly displays the backpack itself visible. Most of all, the MIP displays the objects inside the backpack more clearly, lying on a bin (Figure 3.3b). The white objects are probably harder objects. We identify two cans, presumably deodorant. One half of the lighter is clearly visible, but the igniter is not. The white dots are probably some part of the backpack. A rope is shown, which might part of an earplug headphone. Finally, a box is shown, but the inside of that box cannot be displayed.

3.2.3 Compositing

The compositing technique allows a researcher to color the harder materials more lightly. By trial and error, we came up with a set of parameters at which the backpack is dark green,

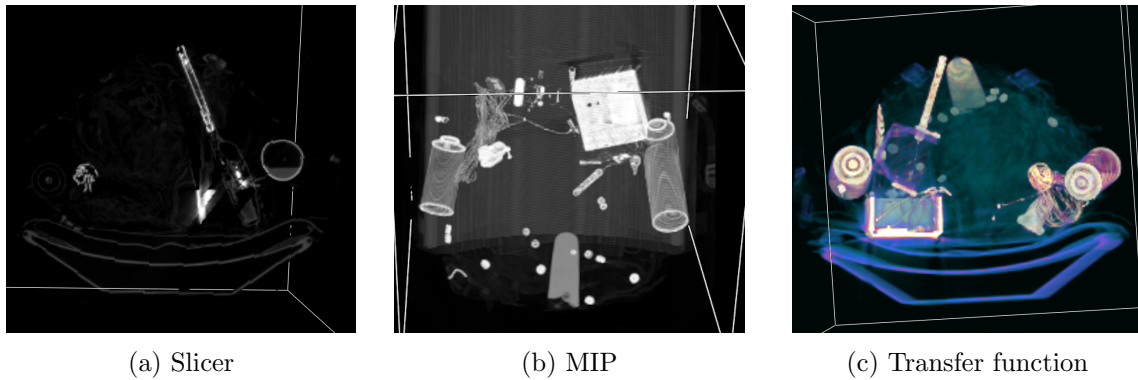


Figure 3.3: Ray casting volume rendering results of a backpack.

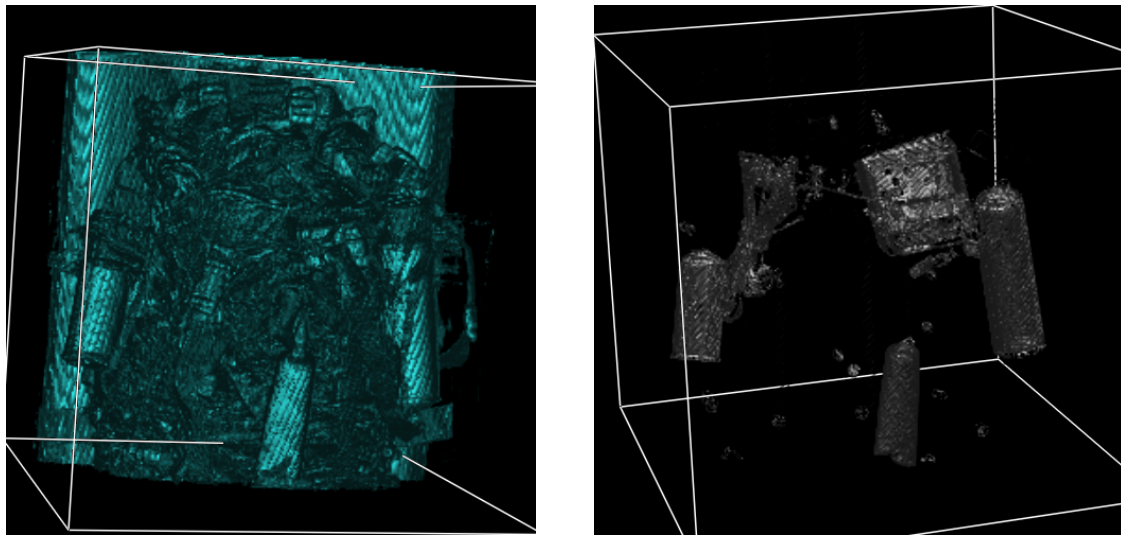


Figure 3.4: 2-D Transfer function volume rendering results of a backpack.

with a low opacity. The objects themselves are colored, but not necessarily better identifiable compared to MIP. An improvement is that the inside of the little box is now visible, but the items inside are not identifiable. Giving lower intensities a higher opacity did not give the desired result because the air around the backpack is also colored at that point. Adjusting the parameters such that the plate become invisible is harming the visibility of the objects inside that backpack. We tried different other settings, but none were more satisfying than the ones showed in Figure 3.3c. The parameters can be found in the appendix.

3.2.4 2-D transfer function

The parameters of the 2-D transfer function makes it possible to view the surface of the backpack itself, when adjusted properly (Figure 3.4a). It seems that the cans, or bottles, are

not inside the backpack, but outside. The backpack is not so big and typical for small travels. If we set the parameters in a specific way, we can also identify the surface of the different cans, a tube, some wires (presumably for ear buds) and a little box (Figure 3.4b). Compared to the known attributes in the backpack, the 2-D transfer function does not add much. The used parameters can be found in the appendix.

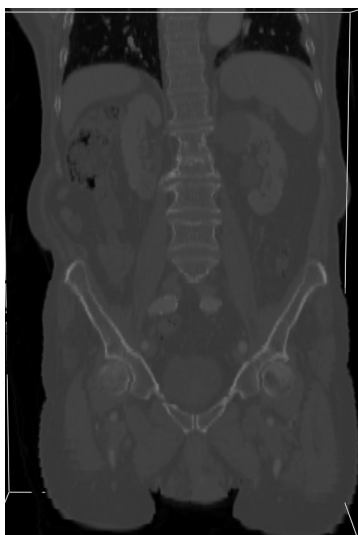
3.2.5 Main findings

The backpack contains some objects that are seem rather harmless: a tube of glue or toothpaste, a pair of ear buds and a box with unidentifiable objects. A rather important finding is the combination of a lighter and a can of deodorant. When this backpack is scanned for security reasons, it is recommended to remove one of these objects from the backpack. Deodorant is flammable and can be used as a weapon or to ignite a fire. When the owner is asked to remove the lighter from the backpack, the safety guard can use that situation to check what is inside the metal-like box.

3.3 Torso

3.3.1 Slicer

The slicer displays a clean cut through a human body (Figure 3.5a). Different parts of the body can be distinguished, like the spine, hips, legs and kidneys. Not all parts are visible, since the slicer only shows the middle slice.



(a) Surface of the items inside the backpack



(b) Surface of the backpack

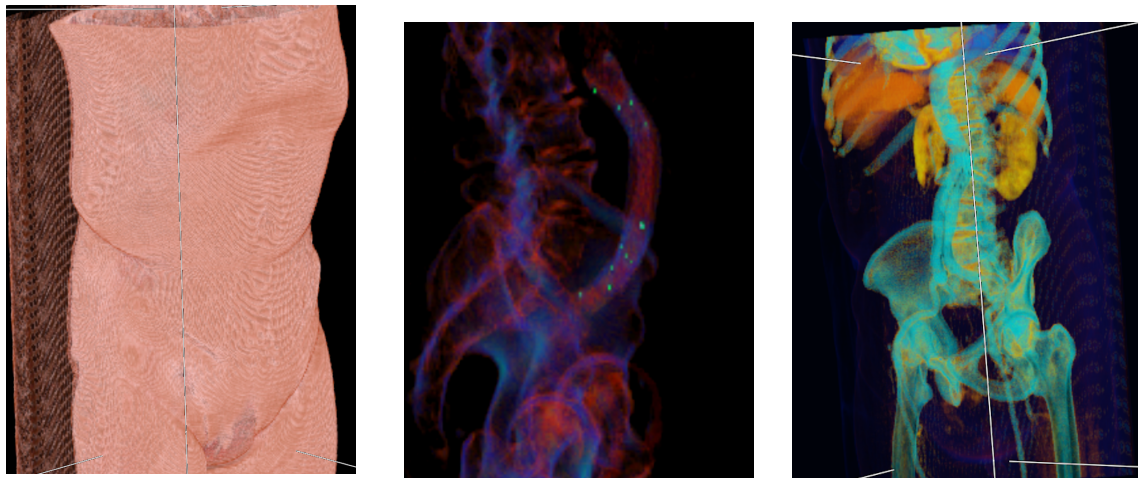
Figure 3.5: 2-D Transfer function volume rendering results of a backpack.

3.3.2 MIP

The MIP shows the maximum value of every ray from the viewer through the object. Therefore, it makes sense that in this case the skeleton of the torso is the main eye catcher (Figure 3.5b). Furthermore, a tube shaped object is shown in what appears to be the belly of the torso. Some spots on the tube are lit, suggesting a material that is harder than bone.

3.3.3 Compositing

The compositing technique makes it possible to go deeper into the different layers and substances in the torso. First of all, it is possible to look at the outside of the torso, when the parameters are adjusted such that the softer tissues are less opaque (Figure 3.6a). Secondly, it is possible to zoom in on the harder materials in the torso. Figure 3.6b shows the skeleton and the hard tube, also displayed in with the MIP. The raster-like structure is now visible, and the fact that the tube surrounds a softer tissue. The tube also contains some hard dots, indicated green in Figure 3.6b. Thirdly, we can set the parameters such that we get more insight in the different organs Figure 3.6c. The organs have a different hardness and are therefore distinguishable with different colors. The different parameter sets can be found in the appendix.



(a) Compositing, showing the skin (b) Compositing, showing a stent (c) Compositing, showing organs

Figure 3.6: Ray casting volume rendering results of a torso.

3.3.4 2-D transfer function

It has to be noticed that the data set of the torso is significantly bigger than the piggy bank and backpack. This is noticeable when it comes the the responsiveness of the 2-D transfer function. It also takes a while before the application has calculated the gradient value of every voxel. But the results, when the parameters are set in a proper way by trial and error, are good looking. Again, the parameters can be set to show either the inside, or the outside of the torso. The shading effect gives a nice representation of the outside of the torso Figure 3.7a. Also, the bone structure can be nicely represented Figure 3.7b. The different organs, however cannot be nicely represented by this technique. The intensities are too closely related to the skin intensity, so the skin will "block" the view of the different organs. The parameters can be found in the appendix.

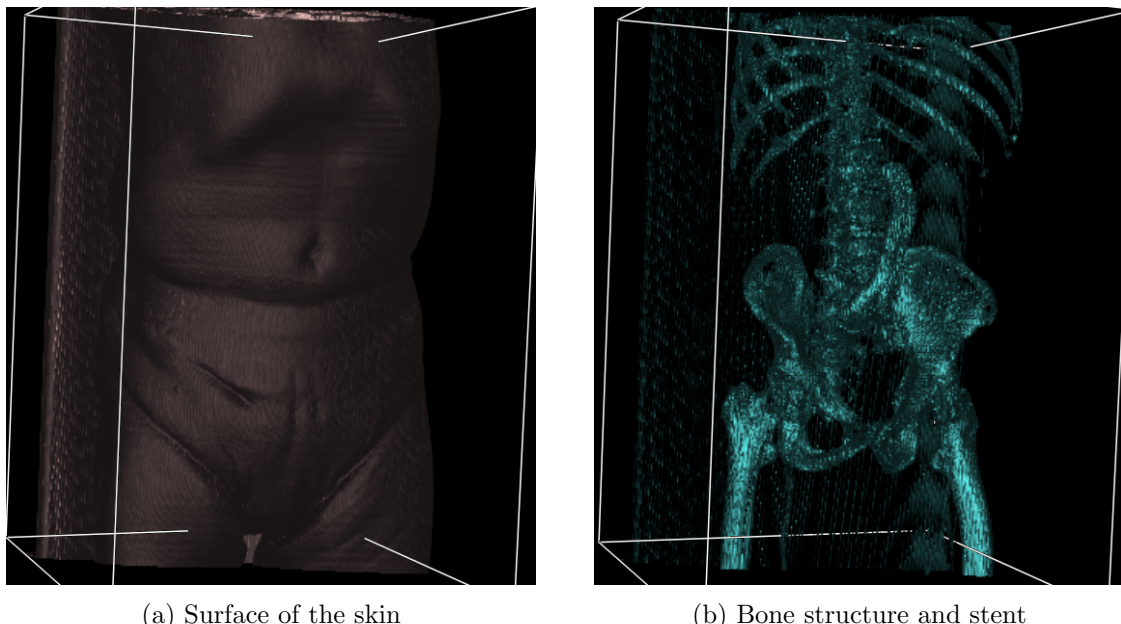


Figure 3.7: 2-D transfer function volume rendering results of a torso.

3.3.5 Main finding

This person has a stent inside her body. Some online research and the consult of a medical student (Smits, L) led us to believe that the object is a multi-branched stent inside the aorta abdominalis. A stent is a tube inserted into a vessel to keep the passageway open. The light spots are short sub-branches of the stent to different smaller veins. This should be taken into account when she will undergo future medical surgery. Furthermore, the torso is probably of a male who is wearing underpants, indicated by small hips and a manly body structure. The liver, kidneys and stomach are clearly distinguishable. The other parts of the belly are harder to visualize. This is probably due to the fact that the intensity is quite the same for the intestines as for the skin.

Chapter 4

Results & Conclusion

We developed different volume rendering techniques and tested them on different data sets. Each technique clearly has pro's and cons. To get all useful information out of a data set, a combination of several techniques is often necessary. A general ranking of the different techniques is therefore not reasonable. However, the different techniques can be ranked on different performance indicators. We therefore ranked the techniques on performance indicators "visibility of surface", "distinguishable items", "showing bigger picture", "responsiveness", "view control", elaborated in the introduction. The results are given in Table 4.1

Table 4.1: Rating of volume rendering techniques on different performance indicators.

Technique	Visibility of surface	Distinguishable items	Showing bigger picture	Responsiveness	View control
Scanner	Low	Medium	Low	High	Low
MIP	Low	High	Medium	Medium/high	Medium/high
Compositing	Medium/high	High	High	Low/medium	High
2-D Transfer function	High	Medium/high	High	Low	Medium/high

When a volume data set is to be explored, one can best start by scanning it with the slicer technique, since it give the user a quick overview of the data. When the data set is more complex, and consisting out of multiple objects of different substances, the slicer is not sufficient. The MIP can offer a solution, by showing most of the distinguishable items in a relatively responsive way. For more in depth knowledge about the big picture, the user should use the compositing technique. This will give the user much more view control and provides the bigger picture, without sacrificing too much responsiveness. This technique often gives the user the best result for creating images to assimilate in a research paper. When the user has even more questions about the data set, especially about the surface of the object(s), he/she could use the 2-D transfer function feature. This will give the user a clear view of the surface of what the data represents, but it takes a lot of time due to the high computational delays.

Chapter 5

Discussion

The results provide a clear overview of the performance and usability of the different volume rendering techniques. However, not all visualization techniques are covered and tested in this paper. Further research can be conducted on the existence of other visualization techniques, and the evaluation of them. Furthermore, while the developed application gives the desired results and steps has been taken to improve the responsiveness, the application's performance is not astonishing. In future development, optimization of the responsiveness performance should be highly prioritised. Furthermore, the results can be influenced by the way that we developed and implemented the different techniques. This would lower the validity and could lead to an misleading conclusion. To prevent this, we checked our code with several teachers of Eindhoven Technical University, who approved the results. This way we made sure that the validity of this research is sufficient. Lastly, the reliability of this research has been taken into account, since all steps to do the research are carefully explained and written down. A researcher is able to follow these steps and check our findings. This makes the reliability sufficient as well.

Chapter 6

Appendix

6.1 Parameter settings

The parameter settings to create the provided images are shown in the figures below. They are reproducible for everyone that has the applications' code.

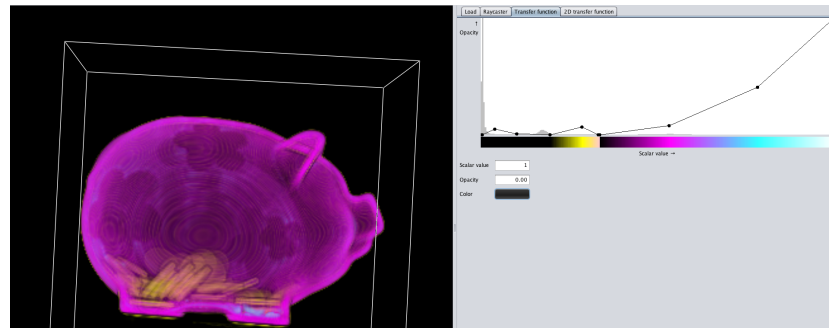


Figure 6.1: Parameters piggy bank 1

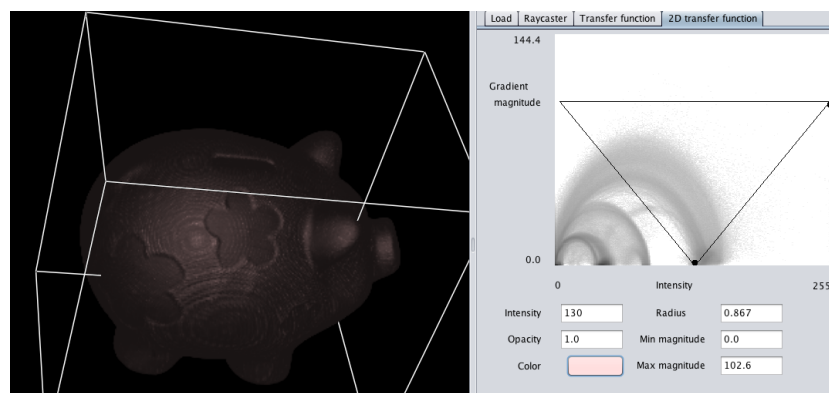


Figure 6.2: Parameters piggy bank 2

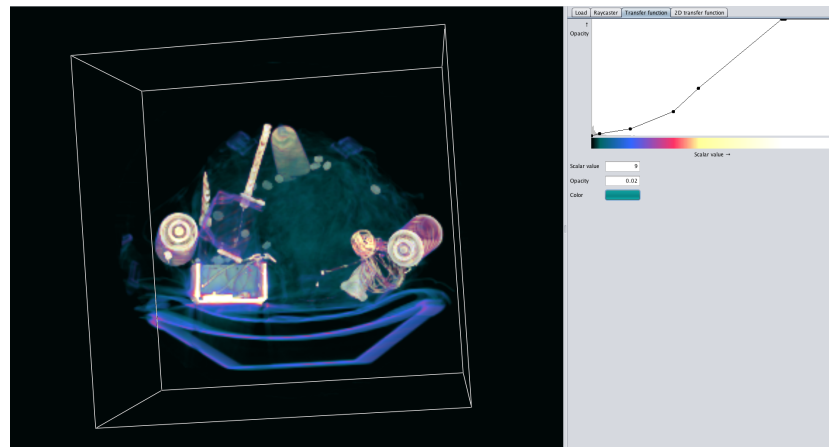


Figure 6.3: Parameters backpack 1

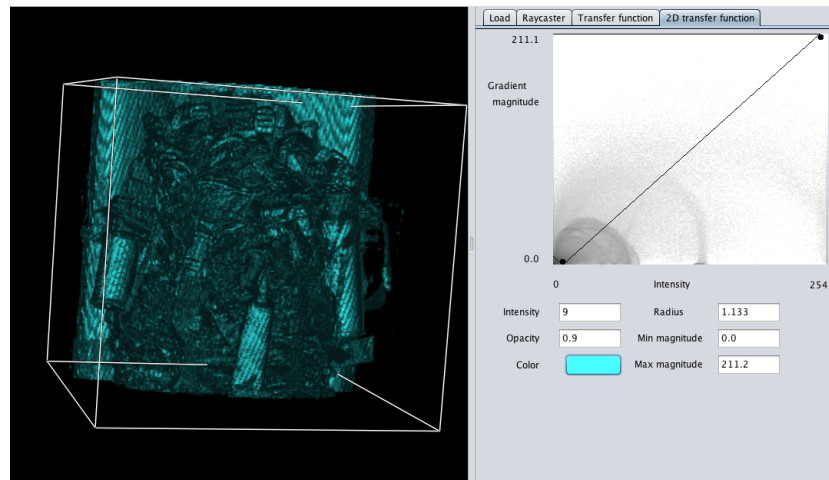


Figure 6.4: Parameters backpack 2

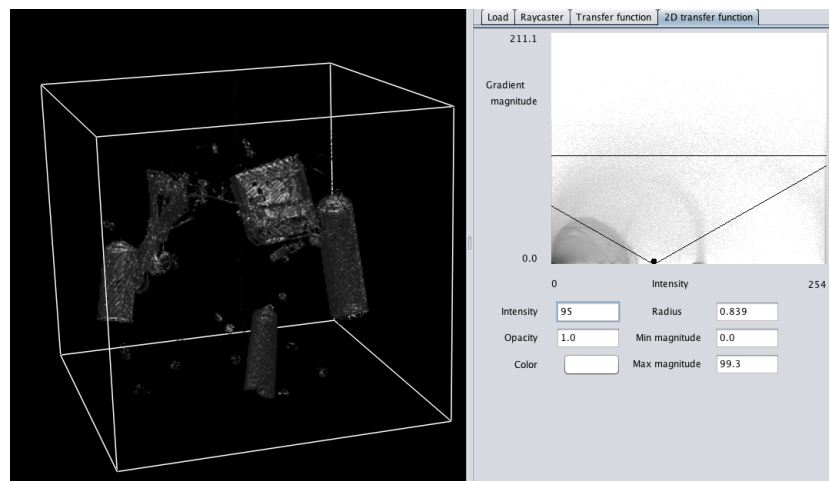


Figure 6.5: Parameters backpack 3

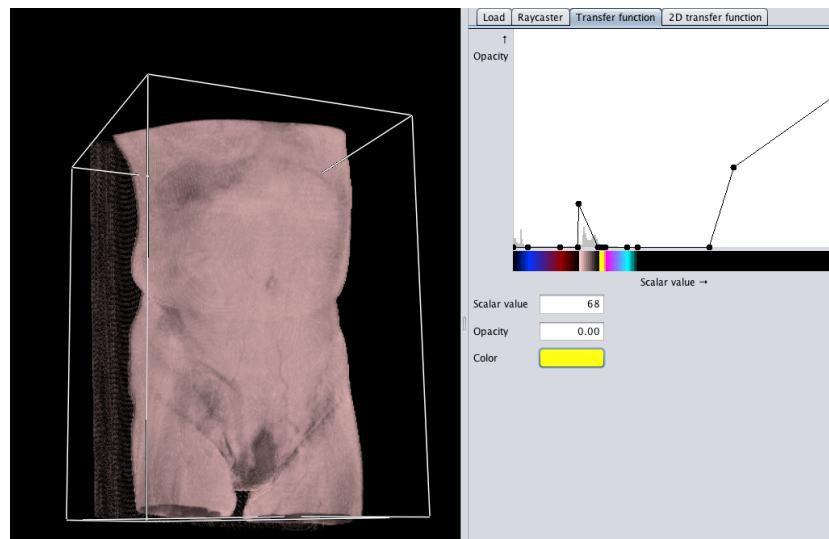


Figure 6.6: Parameters torso 1

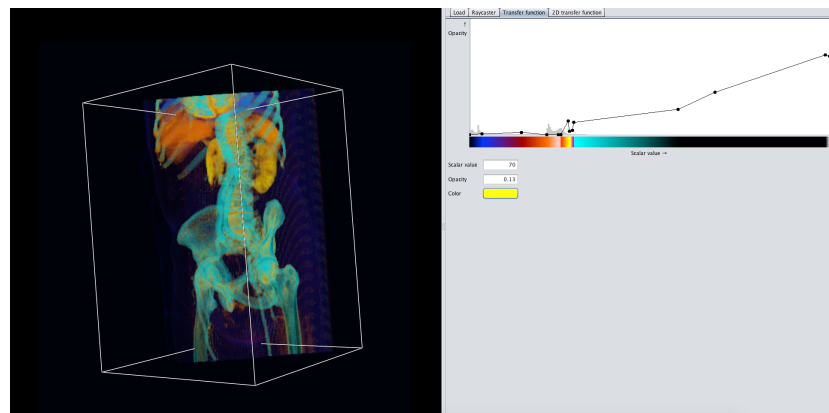


Figure 6.7: Parameters torso 2

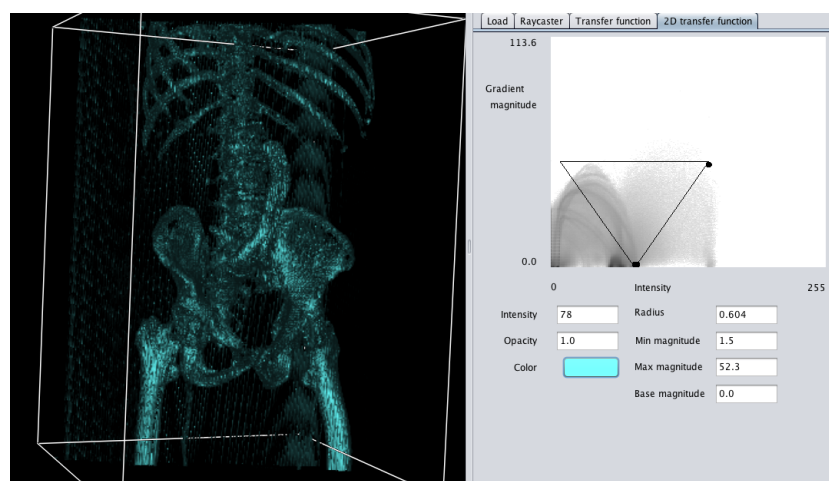


Figure 6.8: Parameters torso 3

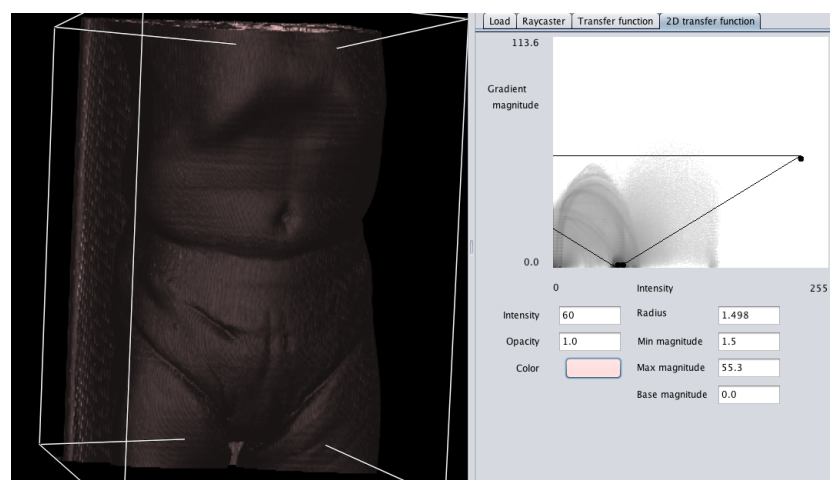


Figure 6.9: Parameters torso 4

Bibliography

- [1] Kierzkowski D., Nakayama N., Routier-Kierzkowska A.L., Weber A., Bayer E., Schorderet M., Reinhardt D., Kuhlemeier C., Smith R.S. (2012). Elastic domains regulate growth and organogenesis in the plant shoot apical meristem.
- [2] Meißner, M., Pfister, H., Westermann, R., & Wittenbrink, C. M. (2000). Volume visualization and volume rendering techniques. Eurographics tutorial.
- [3] Levoy M. (1988). Display of surfaces from volume data. IEEE Computer Graphics and Applications, 8(3):29–37.
- [4] Kniss J., Kindlmann G. L., Hansen C. D. (2002). Multidimensional transfer functions for interactive volume rendering. IEEE Trans. Visualization and Computer Graphics, 8(3):270–285.
- [5] Truernit E., Bauby H., Dubreucq B., Grandjean O., Runions J., Barthélémy J., Palauqui J.C. (2008). High-resolution whole-mount imaging of three-dimensional tissue organization and gene expression enables the study of phloem development and structure in *Arabidopsis*. Plant Cell 20: 1494–1503.
- [6] Roeder A.H.K., Cunha A., Burl M.C., Meyerowitz E.M. (2012). A computational image analysis glossary for biologists. Development 139: 3071–3080.
- [7] Wikipedia, Phong reflection model. https://en.wikipedia.org/wiki/Phong_reflection_model.